Received: 27 February 2022 | Revised: 02 April 2022 | Accepted: 10 April 2022
DOI: 10.22034/ecc.2022.335382.1391
Eurasian Chemical Communications
SAMI

FULL PAPER

Determination of catechol by continuous flow injection analysis via turbidmetric utilizing NAG-4SX3-3D analyzer

Sarah Faris Hameed* | **Nagham Shakir Turkie**

[a]*Department of Chemistry, College of Science, University of Baghdad, Baghdad, Iraq*

A simple and effective technique for detecting catechol by the generation of white precipitate utilizing the reaction of potassium dichromate with catechol in sulfuric acid medium, which is characterized by its speed and sensitivity. The NAG-4SX3-3D analyzer was utilized to measure the incident light attenuation impacting on the precipitate surface grains to quantify turbidity (0-180 degree), the snow led [LED] (blue band 400-480 nm, green band 443-600 nm, and red band 660-697 nm) was utilized to irradiate precipitate particles throughout the processes to get a transducer energy response in mV vs. time. The appropriate parameter was researched in order to increase the sensitivity of the newly devised technique. For catechol measurement, the linear range (0.01-27) millimol.L^{-1} with (r=0.9996), (correlation coefficient), percentage linearity (R^2 percent=99.9۲), and RSD % for the repetition (n=6) were significantly lower than 0.2 percent (0.7, 15 millimol .L^{-1}), with L.O.D. = 154.14 ng/sample from the progressive dilution across the calibration graph's lowest concentration linear dynamic range. The suggested strategy was compared to the traditional method (UV-spectrophotometric at λ_{max}=275 nm and turbidimetric method). It may be concluded that in addition to the technique's sensitivity (developed) and the employment of few chemicals, the approach is also characterized by a dynamic system, which prevents precipitated particle setting during measurements as compared to the conventional reference method's 10 mm irradiation. In addition, continuous dilution in CFIA allows for dealing with high or low concentrations, allowing for a wider range of applications. Based on the foregoing, the developed technique is deemed to be the most appropriate for catechol molecules when compared to the reference methods.

***Corresponding Author:**
Sarah Faris Hameed
Email: sarahf.hameed@yahoo.com
Tel.: +07706234541

KEYWORDS

Catechol; turbidity; continuous flow injection analysis.

Introduction

Aromatic organic compounds are common in natural water bodies and industrial wastewater and they have harmful health and environmental effects [1]. Catechol [Cat] as displayed in Figure 1, 1,2-dihydroxybenzene, 1,2-benzediol, and pyrocatechol. Reinsch was the first to acquire this compound via dry distillation of catechin in 1839. It may be found in plants (onion, eucalyptus, and crudebeetsugar), coal, and tobacco smoke. It has sparked concern because of its widespread existence in nature and potential for human harm. It's used as an anti-fungal agent on seed potatoes and as an antioxidant

in the rubber, dye, pharmaceutical, and oil industries, as well as on seed potatoes [2]. It's also a vital stage in the aerobic degradation of aromatic chemicals that bacteria produce. Catechol is a carcinogenic compound which has a negative impact on the central nervous system [3] which decreases the speed of DNA replication and causes chromosomal aberrations in both animals and humans [4]. It's a colorless crystalline solid (monoclinic crystals) [5] that discolors when exposed to light and air. Water and hydrophobic organic solvents (ethanol and acetone) dissolve it easily [6]. Cat may be found in a wide range of applications. Photography, coloring fur, rubber and plastic manufacture, insecticides, and pharmaceutical sectors all employ it as a reagent [7,8]. There are many techniques to determination of catechol such as electrochemical determination [9], highly selective colorimetric determination [10], carbon electrode [11], and continuous flow injection analysis [12].

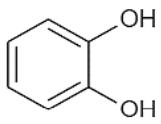

catechol

FIGURE 1 Structure of catechol

Experimental

Chemicals

All of the chemicals used were analytical reagent grade and the solutions were made using distilled water. A standard solution 0.2 M of Cat (C_6H_4 $(OH)_2$ with molecular weight 110.1 g.mol^{-1}, BDH) was prepared by dissolving 11.0100 g in 500 mL of distilled water. A standard solution of potassium dichromate $K_2Cr_2O_7$ with molecular weight 294.22 g.mol^{-1} Hopkin and Williams LTD) was prepared by dissolving 18.3888 g in 250 mL of distilled water.

Apparatus

A flow cell created from a handmade NAG-4SX3-3D analyzer was used to collect the output from the attenuation of incident light (0–180°), as depicted in Figure 2A. The output signals were recorded using a potentiometric recorder (Siemens, Germany), Ismatic peristaltic pump with sample loop and six-port injection valve (Teflon, variable length), A UV spectrophotometric (Shimadzu, Japan), and turbidimetry instrument were used for the traditional methods.

Methodology

The manifold design for determining aromatic organic compound (Catechol) was established via the formation of precipitation particles with potassium dichromate as shown in Figure 2A. It is composed of two lines manifold system which was used as fitted to NAG-4SX3-3D analyzer [13]. The system is equipped with sample segment introduction unit (injection valve with load injection position), where a specified amount can be injected repeatedly with perfect reliability. The first line supplies (distilled water) as a carrier stream which carry the sample zones of catechol 24 mmol.L^{-1} with 175 µL as a sample volume to meet with potassium dichromate in the second at 2.8 mL.min^{-1} flow rate for each line by Y-junction point prior it is introduced to the NAG-4SX3-3D analyzer. The response was recorded by x-t potentiometric record output to measure transducer energy response for the attenuation of the incident light on particles surfaces of precipitate, i.e. white color precipitate. The snow led [LED], which was composed of three mixed bands (blue band from 400-480 nm, green band from 443-600 nm, and red band from (660-697 nm) was used for irradiation of precipitate particles throughout the reactions to obtain transducer energy response in mV versus time. Each solution was assayed triplicate. A proposed mechanism for oxidation of catechol by potassium dichromate is suggested in Scheme

1 [14,15]. Figure 2B displays the repeated successive measurements for NAG-4SX3-3D analyzer transducer output Yz (mV) versus t_{min} (d_{mm}) for 24 mmol.L^{-1} of catechol drugs. Synchronization of system outputs are shown clearly (regarded by the anther as a New approach in NAG-4SX3-3D analyzer.

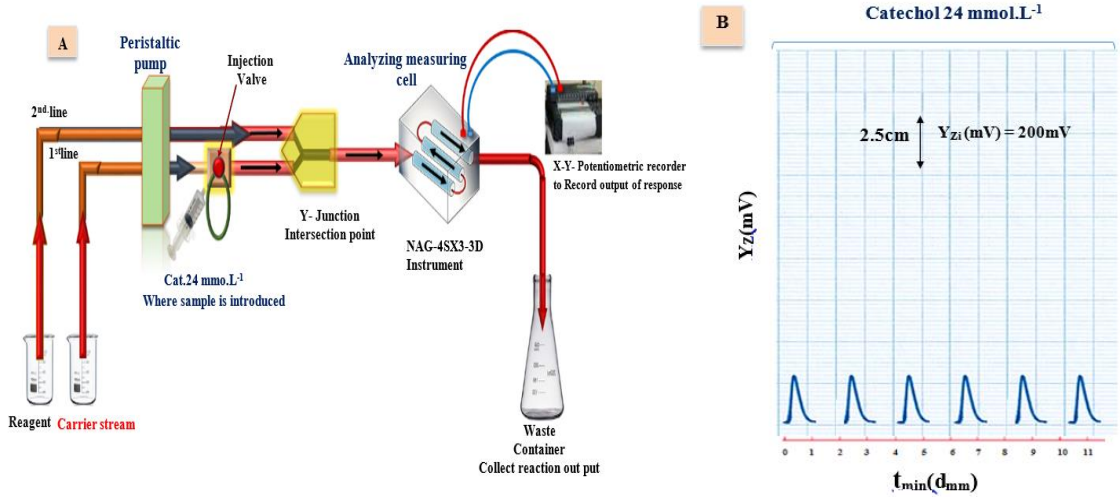

FIGURE 2 A: Diagram of manifold used for assessment NAG-4SX3-3D via reaction of Cat. 24 mmol.L^{-1} with Potassium dichromate 50 mmol.L^{-1} to form white precipitate. B: Profile of preliminary repeated experiments for assessment NAG-4SX3-3D instrument via reaction catechol with Potassium dichromate to form white precipitate

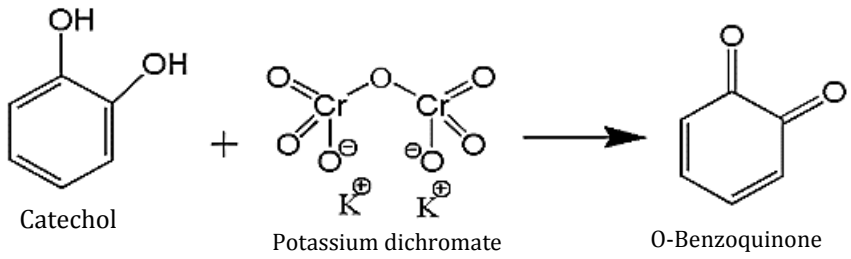

SCHEME 1 Proposed reaction for Cat.-$K_2Cr_2O_7$ system

Result and discussion

The flow injection manifold system Figure 2A was used to examine chemical and physical parameters in order to find the conditions which would produce the reaction product white precipitate with the maximum repeatability and sensitivity. The best way to optimize these variables was to hold them all constant while altering one at a time.

Chemical variables

Effect of variable concentration of potassium dichromate

A series of potassium dichromate solutions were prepared by diluting the stock solution with distilled water to obtain concentrations ranging from (10–150) mmol.L^{-1}, the measurements were performed under the following conditions: cat. (24 mmol.L^{-1}), sample volume of 175 µL, open valve mode, and a flow rate of 2.8 mL/min^{-1} for carrier stream , distilled water and reagent for each line; each measurement was repeated three times. The response profile for this study, as illustrated in figure 4, indicates that the energy transducer response varies with potassium dichromate concentration utilizing the NAG-4SX3-3D analyzer.

It was noticed that when using various concentrations of reagent potassium dichromate from (30 to 150) mmol.L^{-1}, an increase in the response height of precipitate

species with an increase in the concentration of potassium dichromate, which led to an increase in the attenuation of incident light until 130 mmol.L^{-1}, the S/N energy transducer response will decrease; this might be attributed to the dispersion of precipitate particulate with the increase of potassium dichromate up to 130 mmol.L^{-1}. Therefore, 130 mmol.L^{-1} was chosen as the optimum concentration for potassium dichromate. The result obtained was reported in Table 1A, while Table 1B illustrates the segmentation pattern for selection of the optimum segment of Cat. Systems, segment S_2 (i.e., 70-130 mmol.L^{-1}) was used for the Catechol–$K_2Cr_2O_7$ system.

TABLE 1 A: Effect of potassium dichromate concentration on precipitation of Cat. B: Segmentation pattern intercept –slope, correlation coefficient and angle with selection of optimum segment for Cat.-[$K_2Cr_2O_7$] reaction system

(A)

[$K_2Cr_2O_7$] mmol.L^{-1}	$\bar{Y}_{Zi}$(mV) average (n=3)	RSD%	Confidence interval at 95% $\bar{Y}_{Zi}$(mV)± t SEM
30	88	2.86	88±6.260
50	232	1.03	232±5.913
70	448	0.47	448±5.267
100	1528	0.17	1528±6.385
130	2100	0.09	2100±4.919
150	1900	0.12	1900±5.739

(B)

Segment	[$K_2Cr_2O_7$] range mmol.L^{-1}	Intercept mV	Slope mV/ mmol.L^{-1}	correlation coefficient	angle
S_1	30-70	-194.00	9.00	0.993	83.660
S_2	70-130	-1394.67	27.53	0.985	87.920
S_3	100-150	784.00	8.36	0.725	83.177

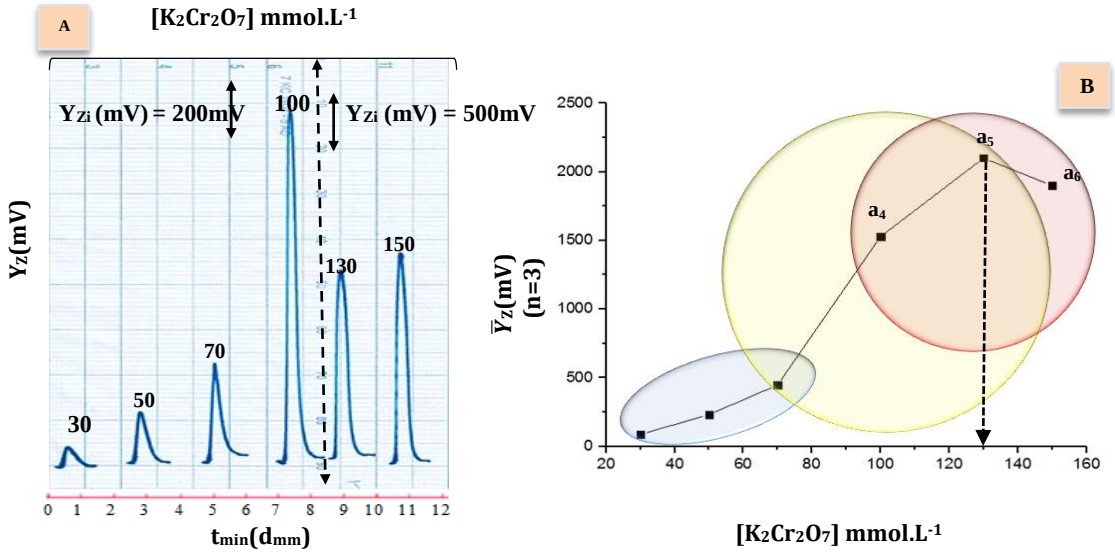

FIGURE 3 A: Response profile of potassium dichromate concentrations effect. B: $\bar{Y}$Z i (mV) output of (S/N) energy transducer response and three data point as one segment with optimum choice.

Effect of different medium (salts and acids)

Using chosen conditions for the Catechol system, Cat. 24 mmol.L^{-1}-$K_2Cr_2O_7$ 130 mmol.L^{-1}, and sample volume of 175µL. The flow rate was 2.8 mL/min^{-1}. The effect of various solutions was used as a carrier stream and was

studied, as well. Different solution medium (CH_3COOH, Tartaric acid, Ascorbic acid, HCl, HNO_3, H_2SO_4, KCl, CH_3COONH_4, NH_4Cl, $NaNO_3$, NaCl, and Na_2CO_3) 50 mmol.L^{-1} concentration in addition to the aqueous medium (distilled water). From Figure 4, it is evident that the studied media cause a decrease in S/N-response. This might be attributed to an increase in agglomeration, i.e., increasing the density of aggregate and compactness with each other. This leads to an increase in the intensity of incident light as there will be more empty spaces among agglomerates of particulate except for H_2SO_4, which leads to an increase in S/N response because of the effect of tiny solid particulate formation that causes a decrease in inter-spatial distances and increases the attenuation of incident light. For the proposed study, H_2SO_4 medium was chosen as the optimum carrier stream for catechol because H_2SO_4 was suitable for the sensitivity and obtained a higher response. Table 2 summarizes the obtained results.

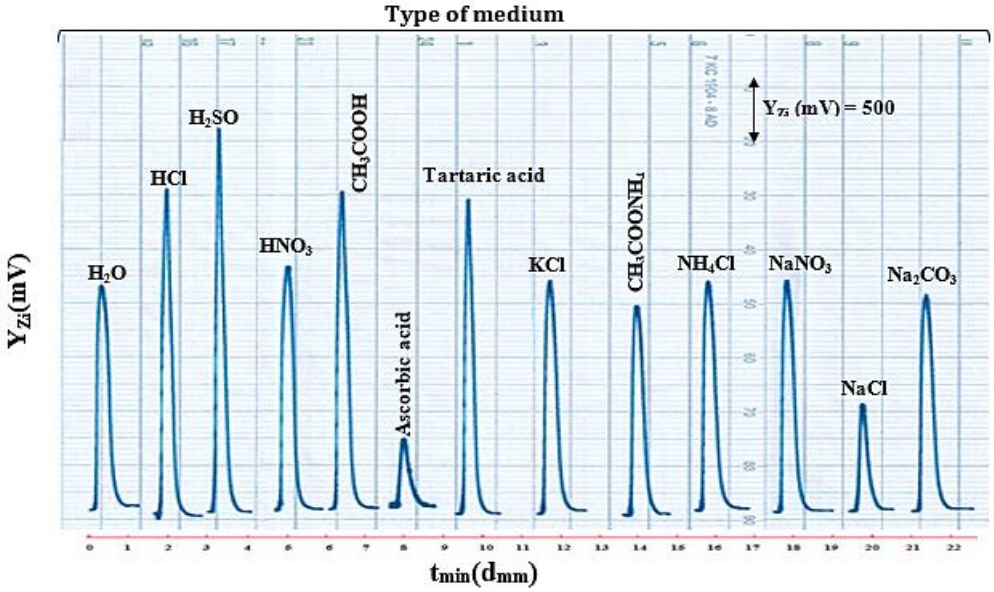

FIGURE 4 Effect of Type of medium (salts & acids) on response profile Y_{Zi}- $t_{(min)}(d_{mm})$

TABLE 2 Effect of different medium precipitation of Catechol (24 mmol.L^{-1} - $K_2Cr_2O_7$ (130 mmol.L^{-1}) system

Type of medium 50 mmol.L^{-1}	$\bar{Y}_{Zi}$(mV) average (n=3)	RSD%	Confidence interval at 95% $\bar{Y}_{Zi}$(mV)± t SEM
Acid			
H_2O	2100	0.09	2100±4.٧٩٥
CH_3COOH	2960	0.07	2960±5.391
Tartaric acid	2940	0.07	2940±5.267
Ascorbic acid	656	0.30	656±4.919
HCl	3080	0.06	3080±4.447
HNO_3	2280	0.11	624±6.285
H_2SO_4	3570	0.05	3570± 4.670
Salt			
KCl	2160	0.09	2160± 4.894
CH_3COONH_4	1960	0.10	1960±4.695
NH_4Cl	2140	0.10	2140±5.267
$NaNO_3$	2160	0.12	2160±6.285
NaCl	1000	0.30	1000±7.403
Na_2CO_3	2020	0.16	2020±7.974

Effect of H_2SO_4 concentration

A series of solutions were prepared ranging from 10 to 100 mmol.L^{-1}. Using a preliminary concentration of catechol 24 mmol.L^{-1} with a sample volume of 175 µL, a flow rate of 2.8 mL.min^{-1}, an open valve mode and a reagent concentration ($K_2Cr_2O_7$) of 130 mmol.L^{-1}. Each measurement was repeated three successive times; this led to an increase in the attenuation of the incident light with an increase of H_2SO_4 concentration. This was due to the form of small-sized particulate, especially if it could be in the form of a nucleus, which in turn collected in its packed blocked form and that will help in agglomeration. This will lead to an increase in the attenuation of incident light of which more than 70 mmol.L^{-1} indicates an increase in small size solubility. 70 mmol.L^{-1} of H_2SO_4 was chosen as the optimum carrier stream.

Table 3A and Table 3B sum up all the obtained result and the application of slope-intercept correlation confident (r) as well as the angle tangent method for determining the optimum segment which was (50-100) mmol.L^{-1} as the optimum.

TABLE 3 A: Effect of variation of H_2SO_4 concentration precipitation of Catechol. B: Segmentation pattern intercept –slope, correlation coefficient and angle with selection of optimum segment for Cat.-[$K_2Cr_2O_7$] reaction system

A			
[H_2SO_4] mmol.L^{-1}	**$\bar{Y}_{Zi}$(mV) average (n=3)**	**RSD%**	**Confidence interval at 95 % $\bar{Y}_{Zi}$(mV)± t SEM**
10	2960	0.08	2960±5.515
30	3340	0.06	3340±5.291
50	3570	0.06	3570±4.894
70	3760	0.05	3760±5.093
100	3400	0.08	3400±6.360

B					
Segment	**[H_2SO_4] mmol.L^{-1}**	**Intercept mV**	**Slope mV/mmol.L^{-1}**	**correlation coefficient**	**Angle**
S_1	10-50	2832.50	15.25	0.990	86.248
S_2	30-70	3031.67	10.50	0.998	84.560
S_3	50-100	3875.79	- 4.08	- 0.570	- 76.225

Physical variables

Flow rate

Using optimum concentration for Cat (24 mmol.L^{-1}) - $K_2Cr_2O_7$ (130 mmol.L^{-1}) - H_2SO_4 (70 mmol.L^{-1}) system with sample volume 175 µL. A variable flow rate was used ranged from (1-4 mL.min^{-1}). The results obtained were proved that 2.5 mL.min^{-1} was chosen for carrier stream and reagent stream. Because it was noticed that at slow flow rates, there were wider in peak base width (Δt_B), as depicted in Table 4A due to dilution and dispersion, followed by decrease of peak height at flow rate > 2.5 mL.min^{-1}, it can be inferred that an increase in the flow rate above 2.5 mL.min^{-1} causes, response irregular because the precipitated particulates are moved faster and take a very short time passing in front of measuring cells. For this, 2.5 mL.min^{-1} was chosen to the optimum flow rate for both carrier stream and reagent line for catechol system. The applications for slope-intercept method was used for choosing the optimum flow rate which should be within the chosen segment which S_2 (2.0-2.8 mL.min^{-1}) to be selected as optimum segments for Catechol as shown in Table 4B.

TABLE 4 A: Variation effect of flow rate on precipitation of Catechol. B: $\bar{Y}Zi$ (mV) output of (S/N) energy transducer response and four data points as one segment with an optimum choice

A									
Pump speed Flow rate for each line	**Flow rate mL.min^{-1}**	**$\bar{Y}_{Zi}$(mV) average (n=3)**	**RSD%**	**Confidence interval at 95% $\bar{Y}_{Zi}$(mV)± t SEM**	**Δt_{sec}**	**V_{add} (mL) at flow rate**	**C (mmo.L^{-1})**	**D.F**	**t_{sec}**
5	1.0	4360	0.04	4360±4.298	204	6.975	0.602	39.8571	120
10	1.5	3700	0.04	3700±3.279	120	6.175	0.680	35.2857	72
15	2.0	4180	0.05	4180±4.919	84	5.775	0.727	33.0000	36
20	2.5	3940	0.05	3940±5.366	66	5.675	0.740	32.4286	60
25	2.8	3720	0.05	3720±5.043	63	6.055	0.694	34.6000	30
30	3.0	3660	0.07	3660±6.012	60	6.175	0.680	35.286	24
35	3.5	3660	0.06	3660±5.739	42	5.075	0.828	92.0000	18
40	4.0	3520	0.06	3520±5.242	42	5.775	0.727	33.0000	18

B					
Segment	**Flow rate mL.min^{-1}**	**Intercept mV**	**Slope mV/ mmol.L^{-1}**	**correlation coefficient**	**Angle**
S_1	1.0-2.0	4350.00	-180.00	-0.264	-89.682
S_2	2.0-2.8	5322.24	-565.31	-0.993	-89.899
S_3	2.8-3.5	3894.62	-69.23	-0.721	-89.172
S_4	3.0-4.0	4103.33	-140.00	-0.866	-89.591

Sample volume

Variation sample volumes (82, 115, 139, 141, 175, and 281 µL) with open valve mode were studied at an optimum flow rate of 2.5 mL/min-1 for the carrier stream and reagent. Catechol concentration (24 mmol.L^{-1}) was chosen. It was noticed that an increase in sample volume led to an increase in the height of the response without having an effect on the response profile up to 175 µL for catechol, Table 5. Above 175 µL, there was either a broadening of the peak maxima and an increase in base width (Δt_B) or a decrease in peak height. This is illustrated in Figure 5 which indicates that the optimum volume was 175 µL for Catechol to a better response profile.

TABLE 5 Effect of the variation of sample volume on precipitation of Catechol

Length of sample segment cm r= 0.5	**Sample volume µL**	**$\bar{Y}_{Zi}$(mV) average (n=3)**	**RSD%**	**Confidence interval at 95% $\bar{Y}_{Zi}$(mV)± t SEM**	**Δt_{sec}**	**V_{add} (mL) at flow rate**	**C (mmo.L^{-1})**	**D.F**	**t_{sec}**
				Cat.					
10.4	82	2660	0.05	2660±3.006	54	3.082	0.639	37.5854	36
14.6	115	3040	0.06	3040±4.770	60	3.615	0.763	31.4348	42
17.7	139	3160	0.06	3160±4.919	66	3.139	1.063	22.5827	36
18	141	3300	0.06	3300±4.546	60	3.141	1.077	22.2766	36
22.3	175	3900	0.05	3900±5.291	60	2.675	1.570	15.2827	30
35.8	281	2320	0.09	2320±5.043	65	5.698	1.184	20.2764	37

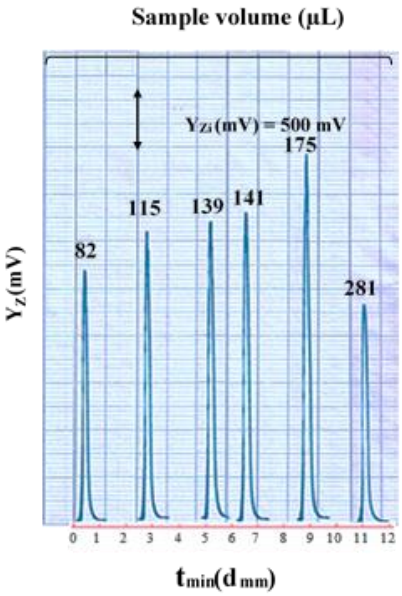

FIGURE 5 Response profile of sample volume on energy transducer response for the assessment of NAG-4SX3-3D via formation of white precipitate

Effect of reaction loop lengths

Variable coil lengths (0-30 cm) were studied. These lengths comprise a volume (0-942 µL) which was connected after Y-junction directly in flow system, as demonstrated in Figure 6. The optimum concentration of Cat. (24 mmol.L^{-1})- 130 mmol.L^{-1} $K_2Cr_2O_4$ -70 mmol.L^{-1} - H_2SO_4 system was used with sample volume 175 µL. The effect of reaction coil length on sensitivity was expressed as an S/N energy transducer response. It was noticed that an increase of coil length causes a decrease in sensitivity, and this might be explained to the production of larger particles, increase particulate weight and spreading it on a wider surfaces area, which in turn lead to a difficulty in passing through flow cell. Hence, reaction coil was avoided for usage in catechol system.

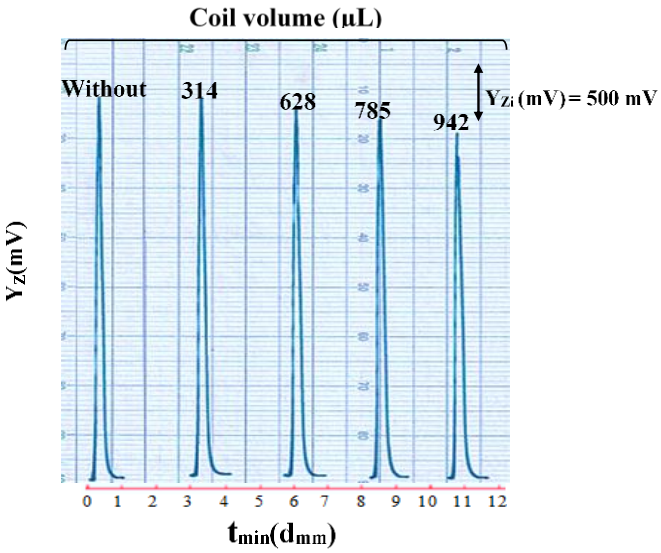

FIGURE 6 the response profile of coil volume on energy transducer response for the assessment of NAG-4SX3-3D by the creation of white precipitate

Study of Y-junction point

The Y- junction plays a main role in the mixing of reactant in the reaction. The Y-junction was connected before measuring cell directly in flow system; its effect on response profile was studied by using variable Y-junction in different parameters is displayed in Figure 7. The optimum concentration Cat (24 mmol.L^{-1}) was used with sample volume 175 µL, while the flow rate 2.5 mL.min^{-1} was applied for both carrier stream and reagent. Figure 7 demonstrates all obtained result profiles of Y- junction (meeting zone) for the effect of S/N transducer energy response. A different volume mixing chambers has been used in addition to intersection point in a larger diameter to study the effect on agglomerate, regulation, and regular distribution for particulate previous to the entrance of the flow tube. However, it causes in decreasing of sensitivity due to particle scattering and its dispersion and increasing the inside spatial distances which cause the diminish capability of preventing the incident light to increase the height of response measurement of the energy transducer, as indicated in Table 6. Therefore, it was believed that removal of premix chamber or intersection point at a larger tube diameter through manifold unit at two entrances at 3 mm (I.D) and the outlet with internal diameter of 3 mm. All that prove the ideal Y- junction for mixing reactant and formation precipitate particles in sulfuring acid medium is 21.2 µL.

TABLE 6 Data set point obtained for Volume of Y-junction & premix chamber in the determination procedure of Catechol

Type of Y-junction		Volume $\pi r^2 h$	$\bar{Y}_{Zi}$(mV) average (n=3)	t_{sec}	Volume mL	C (mm/L) DF
					At junction point	
Intersection junction point	3 mm (ID) 3 mm (thickness)	21.2µL	3900	28	2.5295	1.6604 14.4545
	5 mm (ID) 5 mm (thickness)	98.00 µL	2700	28.5	2.6480	1.5861 15.1314
	14 mm (ID) 12 mm(thickness)	1.85 mL	2780	29	4.4417	0.9456 25.3810
Premix chamber	14mm (ID) 13 mm (thickness)	2.00 mL	2420	30	4.6750	0.8984 26.7143
	14 mm (ID) 14 mm (thickness)	2.15 mL	2600	30.5	4.8667	0.8630 27.8095

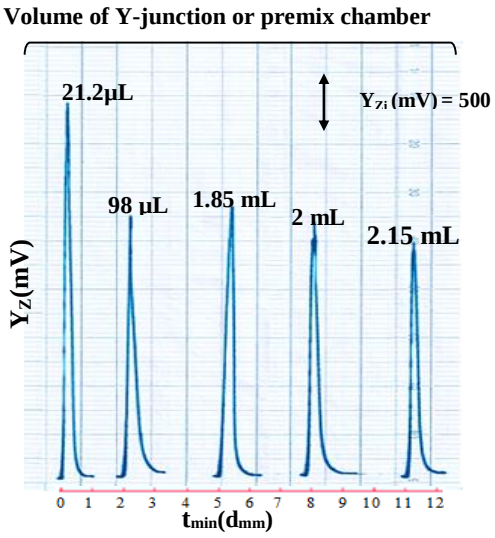

FIGURE 7 Response profile of Yz (mV) - $t_{min}(10_{mm})$ for the assessment of NAG-4SX3-3D analyzer via formation of white precipitate of Catechol

Using a scatter plot, estimate the linear dynamic range of catechol on the S/N energy transducer response.

In previous section, physical as well as chemical variables were set at their optimum values (Cat- $K_2Cr_2O_7$ (130 mmol.L^{-1})-H_2SO_4 (70 mmol.L^{-1}) system, 175 µL sample volume, without delay reaction coil and 2.5 mL.min^{-1} flow rate for both carrier stream and reagent line. A series of solutions for organic compound (0.01-45 mmol.L^{-1}) for catechol were prepared. Each measurement was repeated three times. Transducer energy response of the average peak height (mV) was plotted against the concentration of two organic compounds were obtained. A straight line graph in both Figure 8A and Figure 8B from 0.01-27 mmol.L^{-1} of Catechol was obtained above 27 mmol.L^{-1}. The value for correlation coefficient will decrease and deviate linearity, as indicated in Table 7. This is most probably due to the increase of precipitate particles in front of the detector which might be due to the attenuation in transmitted light. The assessment evaluation of the new developed methodology for the determination of catechol was compared with available reference method [14]; namely spectrophotometric method, as displayed in Figure 10A and turbidity method, as demonstrated in Figure 10B and Figure 10C indicates for catechol, as well. The spectrophotometric method is illustrated in Figure 9 based on the absorbance measurement for variable range of concentration as depicted in table 6 at λmax =275 nm for Catechol.

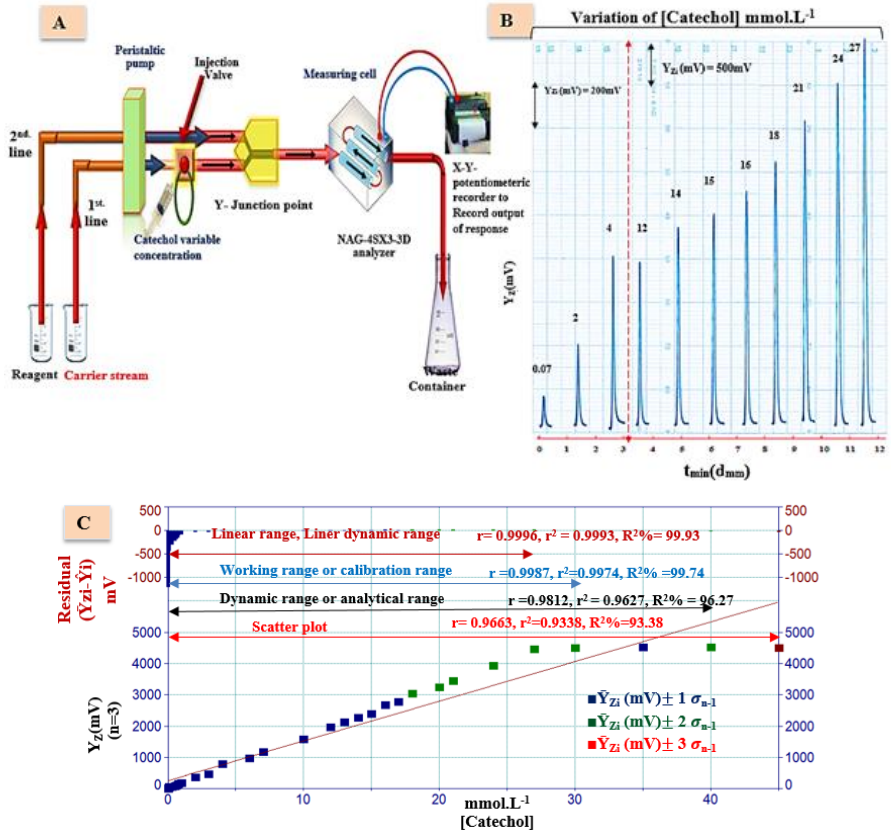

FIGURE 8 A: Flow gram system used for the determination of Catechol. B: Some of profiles versus time, potentiometric scanning speed 1cm.min^{-1}. C: Different range for the effect of Catechol concentration on attenuation of incident light using NAG-4SX3-3D analyzer for: scatter plot range, dynamic range, working range and linear range against response transducer energy in mV, using Catechol – $K_2Cr_2O_7$ (130 mmol.L^{-1}) –H_2SO_4 (70 mmol.L^{-1}) system.

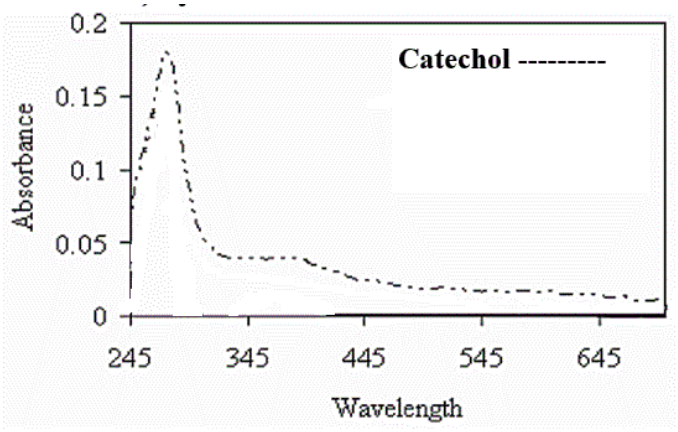

FIGURE 9 UV- Spectrum of Cat. at concentration of 0.03 mmol.L^{-1} that shown at λ_{max} = 275nm

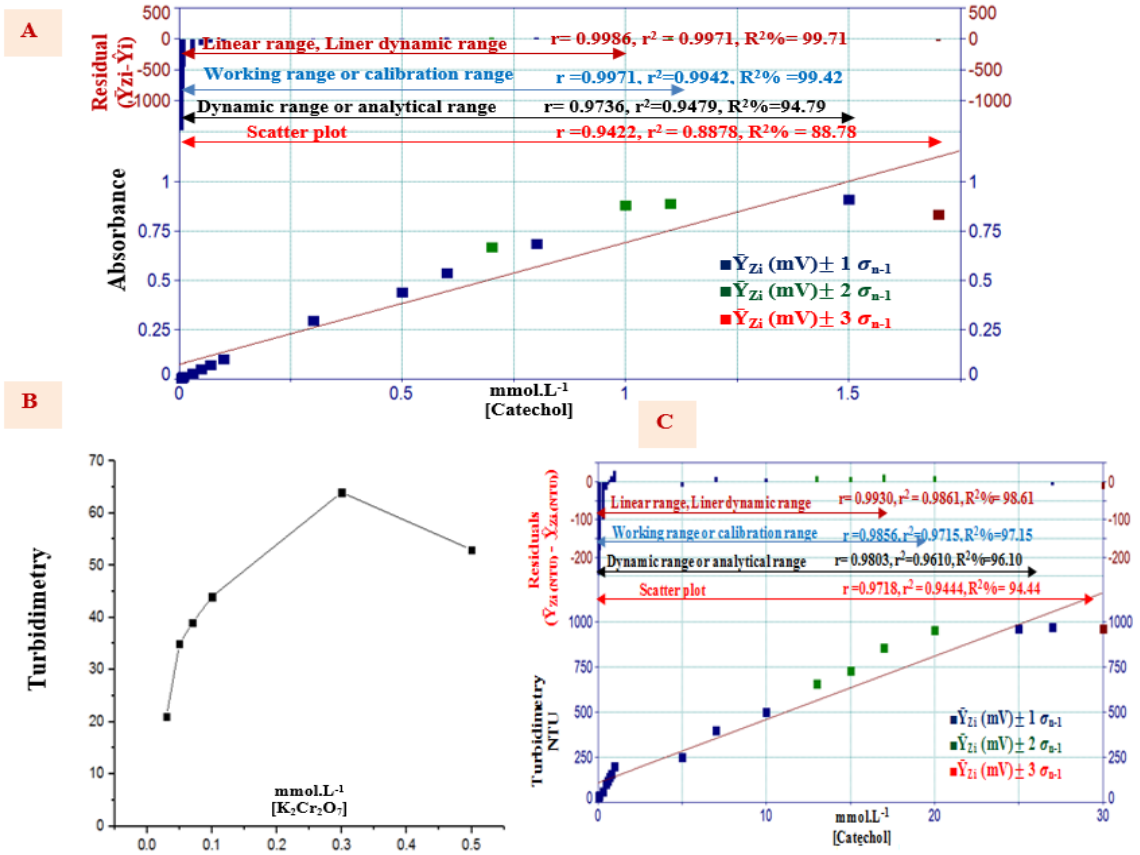

FIGURE 10 A: The scatter plot for [Catechol] using classical method at λmax=275 nm in addition to working, dynamic range and linear; B: Graphical representation shows the optimum concentration of $K_2Cr_2O_7$ reacted with Catechol (5 mmol.L^{-1}) in the presence of the best H_2SO_4 concentration of Turbidimetric method; C: The scatter plot for [Catechol] using turbidimetric method in addition to dynamic range, working range and linear range.

Residual = ($\bar{Y}_{Zi}$(NTU)-$\hat{Y}_{Zi}$(NTU)) in NTU for turbidimetric method, $\bar{Y}_{Zi}$(NTU)= average of practical value in NTU, $\hat{Y}_{Zi}$(NTU) = estimated value in NTU.

TABLE 7 Summary of results for linear regression for the variation of (S/N) energy transducer response with Catechol concentration using first degree equation of the form $\hat{Y}=a+ b x$ at optimum conditions

Type of mode	Range of [Fe (II)] ion mmol.L^{-1}(n)	$\hat{Y}_{Zi}=a \pm S_a t+b(\Delta y/\Delta x_{mmol/L}) \pm S_b t$ [Fe (II)] mmol.L^{-1} at confidence level 95%, n-2	r, r^2, R^2%	t_{tab} at 95%, n-2	Calculated t-value $t_{cal}=/r/\sqrt{n-2}/\sqrt{1-r^2}$
Developed method using NAG - 4SX3 - 3D analyzer					
UV- Spectrophotometer at λ_{max}= 275 nm.					
Turbidity method					
Linear range or linear dynamic range	0.01-27(28)	30.2196±20.7260+162.9733±1.7414 [Cat.] mmol.L^{-1}	0.9996, 0.9993, 99.93	2.056 << 192.356	
	0.005-1(13)	0.0094±0.0147+0.8818±0.0315 [Cat.] mmol.L^{-1}	0.9986, 0.9971, 99.71	2.2010 << 61.628	
	0.05-20(16)	74.6351±26.8115+44.4232±3.0216[Cat.] mmol.L^{-1}	0.9930, 0.9861, 98.61	2.145 << 31.534	
Working range or calibration range	0.01-30 (29)	47.0562±41.5641+159.6001±3.2088 [Cat.] mmol.L^{-1}	0.9987, 0.9974, 99.47	2.052 << 102.054	
	0.005-1.1 (14)	0.0147±0.0220+0.8510±0.0407 [Cat.] mmol.L^{-1}	0.9971, 0.9942, 99.42	2.179 << 45.543	
	0.05-25(17)	86.9907±40.3723+40.6748±3.8341 [Cat.] mmol.L^{-1}	0.9856, 0.9715, 97.15	2.132<<22.612	
Dynamic range or analytical range	0.01-40(31)	172.8565±163.8888+139.2135±10.4050 [Cat.]mmol.L^{-1}	0.9812, 0.9627, 96.27	2.045<<27.364	
	0.005-1.5(15)	0.0447±0.0663+0.7283±0.1022 [Cat.] mmol.L^{-1}	0.9736, 0.9479, 94.79	2.160<<15.385	
	0.05-27(18)	97.2143±48.7352+37.8713±4.0443 [Cat.] mmol.L^{-1}	0.9803, 0.9610, 96.10	2.120 <<19.851	
Scatter plot	0.01-45(32)	261.7196± 219.2967+126.7355±12.5855 [Cat.]mmol.L^{-1}	0.9663, 0.9338, 93.38	2.042<<20.567	
	0.005-1.7(16)	0.0759±0.0952+0.6163±0.1257 [Cat.] mmol.L^{-1}	0.9422, 0.8878, 88.78	2.145 <<10.525	
	0.05-30(19)	109.6029±58.9805+34.9442±4.3371[Cat.] mmol.L^{-1}	0.9718, 0.9444, 94.44	2.1098 <<16.999	

n: no. of measurement, $\hat{Y}_{Zi}$ (mV); estimated response (n=3) in mV for developed method and $\hat{Y}_{Zi}$ = estimated value without unite for spectrophotometric method or in NTU for turbidimetric method, r: correlation coefficient, r^2: coefficient of determination, R^2% (percentage capital R- squared): explained variation as a percentage/total variation and $t_{tab}= t_{0.05}/2$, n-2, volume of measuring cell 1 mL for UV-Sp. and 10 mL for turbidimetric.

The limit of detection (LOD)

The detection limit of Catechol was calculated using three different methods [17], as reported in Table 8.

1-Gradual dilution: It is based on gradual dilution of the lowest concentration in the scatter plot, this should be considered as the trustable and value of D.L.

2-Theoretically: It depends on slope method and is based on the dynamic range, as well.

3-Theoretically method depends on the linear dynamic range due to the low value of residual (Sy/x) which equals to Sb of the form $\hat{Y}= Y_b+ 3S_b$, Y_b(the average response for the blank solution). This is equivalent to intercept (a) in straight line equation y=a+bx.

Repeatability

The measurement of precision achieved by the whole assay process, as displayed in Figure 10 and Table 9, sums up the measurements of two concentration of catechol that each one is repeated for six successive measurements. It shows that the percentage relative standard deviation was less than 0.2%, while Figure 10 illustrates a kind of response profiles for the used concentrations.

TABLE.8 Detection Limit of Catechol using 175 µL as an injection sample and the optimum parameters using Cat (24 mmol.L^{-1})-[$K_2Cr_2O_7$] (130 mmol.L^{-1})- H_2SO_4 (70 mmol.L^{-1}) system

Practically based on the gradual dilution for the minimum concentration in scatter plot		**Theoretical based on the value of slope x=3S_B/slope**	**Theoretical based on the linear equation $\hat{Y} = Y_b + 3Sb$**	**Limit of quantitative L.O. Q $\hat{Y}=Y_b+10S_b$**
Newly developed method (0.008) mmo.L-1	Classical method spectrophotometric method (0.0009) mmol.L^{-1} Turbidmetric method (0.01)mmol.L^{-1}			
154.14 ng/sample	0.0991 µg/ sample 11.01 µg/ sample	0.0674 µg /sample	13.5200 µg/ sample	45.0667 µg/ sample

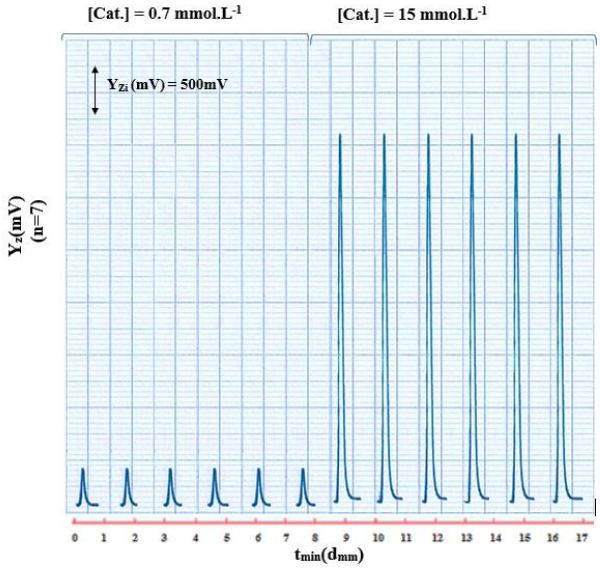

FIGURE 10 Y_Zi (mV) – $t_{(min)}(d_{mm})$ profile of seven successive measurement with a repeatability of profile for 0.7 mmol.L-1and 15 mmol.L^{-1} concentration of [Catechol] using $K_2Cr_2O_7$ (130 mmol.L^{-1})-H_2SO_4(70 mmol.L^{-1}), using 175 µL as injection of sample loop and 2.5mL.min^{-1} flow rate for each line. Also, high measurement repeatability at six high sensitivity of using 25 mm→ 500 mV

TABLE 9 Repeatability of Catechol at optimum parameters with 175 µL sample volume

Concentration of molecule mmol.L^{-1}	**$\bar{Y}_{Zi}$ (mV) average of responses (n=6)**	**RSD%**	**Confidence interval at 95% $\bar{Y}_{zi}$ (mV)± $t_{0.05/2}\sigma_{n-1}/\sqrt{n}$**
0.7	140	0.134	140± 0.1878
15	2400	0.058	2400± 1.3786

Comparison between reference methods already used with newly developed method using the NAG 4SX3-3D instrument, the comparison based on the sensitivity

Under the established optimum conditions Cat.(variable concentration)- $K_2Cr_2O_7$ (130 mmol.L^{-1} system, 175 µL sample volume, 2.5 mL.min^{-1} flow rate, and 21.2 µL Y junction point of continuous flow injection analysis coupled with NAG 4X3-3D Analyzer, the details comparison was made against UV-spectrophotometric at λmax= 275 nm and turbidimetric procedures. Both procedures were compared with the newly developed

method. Two axis were used, one of which is applied for the newly developed procedure that is the Y-axis, while X-axis will represent the classical reference method. The plotted Figure 11A and Figure 11B curve indicate a clear bias for the Y-axis, i.e. directed to the developed method. In addition, the slope angle demonstrates that it is greater than 45° (i.e., 89.68° for comparison between developed method against UV-spectrophotometric, but no significant difference with turbidity method (slope angle ≈ 42°).

It can be inferred that in addition to the sensitivity of the method (developed) and the use of little chemicals, as it also characterized by a dynamic system, this in turn prevents setting of the precipitated particulate during measurements compared with 10 mm irradiation in classical reference method. Likewise, a continuous dilution in CFIA allows dealing with high or low concentration, i.e. the wider range. On the above mentioned facts, the choice of the developed method is regarded as the most suitable as the reference methods for both molecules. The summary of results for calibration graph used linear equation and comparison between different methods for each molecule, as reported in Table 10.

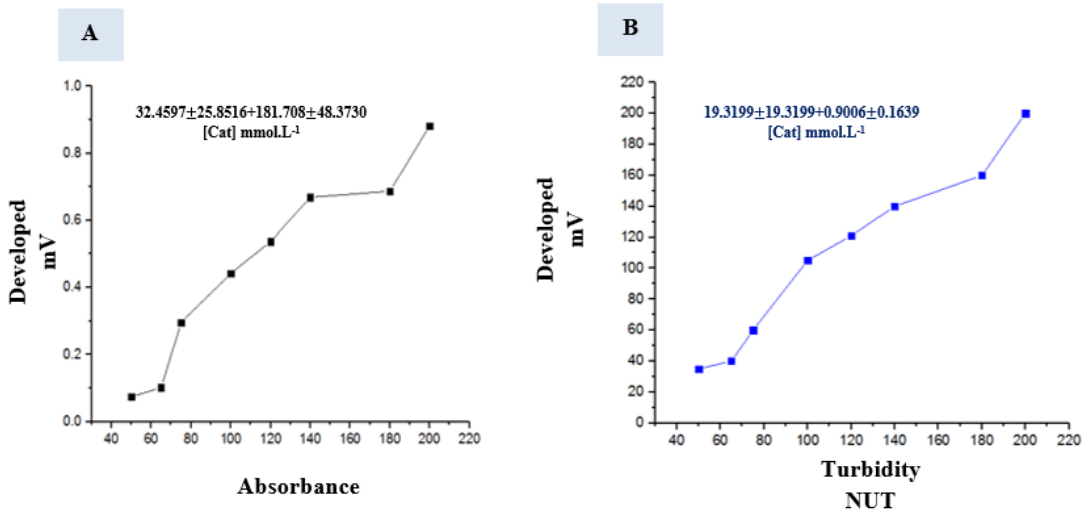

FIGURE 11 A: Energy transducer response expressed as an average peak heights (mV) using NAG-4SX3-3D analyzer and Uv spectrophotometric method at λmax=275 nm. (B): Y predicated ($\hat{Y}_i$) using two method NAG4SX3-3D Analyzer (mV) and classical method (turbidity instrument) NTU

TABLE 10 presents a summary of the findings obtained utilizing various catechol techniques.

Catechol molecule					
Measurements expressed as an average of responses (n=3)					
Developed NAG-4SX3-3D analyzer $\bar{y}_i$(mV)	Classical method		$\bar{y}_{i(Mv)\,/\,dep}$ vs $\bar{y}_{iabs}$ or $\bar{y}_i$(NTu)		[Cat.] mmol.L^{-1} In depended variable (X_i)
	Absorbance at λ_{max}=275 nm $\bar{y}_{iAbs}$	Turbidity $\bar{y}_i$(NTu)	$\hat{y}_{i(dev\text{-}Abs)}$	$\hat{y}_{i(dev\text{-}turb)}$	
50	0.074	35	45.906	50.842	0.07
65	0.102	40	50.994	55.345	0.1
75	0.296	60	86.245	73.358	0.3
100	0.442	105	112.775	113.886	0.5
120	0.537	121	130.037	128.296	0.6
140	0.669	140	154.023	145.408	0.7
180	0.687	160	157.293	163.420	0.8
200	0.882	200	192.727	199.446	1
35.1940±20.511+159.3239±34.9355[Cat] mmol/l	0.2057±0.0357+0.8660±0.0598[Cat] mmol/l	17.2692±9.3094+177.6036±15.6111[Cat] mmol/l	32.4597±25.8516+181.708±48.3730[Cat] mmol/l	19.3199±19.8422+0.9006±0.1639[Cat] mmol/l	Linear regression at confidence level 95% , n-2 $\hat{y}_i = a \pm S_a t + b \pm S_b t$[Cat] mmol/L
0.9759, 0.9524 , 95.24	0.9975,0.9949 , 99.49	0.9959 ,0.9918 , 99.18	0.9663, 0.9337, 93.37 89.68 ◦	0.9838, 0.9679, 96.79, 42.01 ◦	

X: Catechol molecule, ŷZi: in mV for developed method, without unite for UV-Sp method and NTU for turbidity method

Conclusion

The proposed method uses less expensive apparatus and reagents than the traditional methodology.

In this study, the NAG-4SX3-3D analyzer was used to provide a more accurate and faster determination. RSD % for the repetition (n=6) were significantly lower than 0.2 %, indicating that the recommended method is accurate sufficient. This method may also be used to determine catechol and it has the added benefit of achieving high sensitivity without the need of heat or extraction. The statistical analysis yielded results that were similar to those obtained using the traditional method.

Acknowledgements

We would like to express our heartfelt gratitude to Prof. Issam Mohammad Ali Shakir for his superb direction and help in finishing this project and supplying us with all of the essential resources. It has been greatly appreciated and I would like to express my gratitude to Professor Nagham Shakir, who provided significant guidance in developing the research.

Orcid:

Sarah Faris Hameed:
https://www.orcid.org/0000-0002-7607-3498

References

[1] J.A. Garrido-Cardenas, B. Esteban-García, A. Agüera, J.A. Sánchez-Pérez, F. Manzano-Agugliaro, *Int. J. Environ. Res.*, **2019**, *17*, 170. [Crossref], [Google Scholar], [Publisher]

[2] C. Tudisco, M.T. Cambria, G.G. Condorelli, , **2018**, 335–370. [Crossref], [Google Scholar], [Publisher]

[3] A.J. Li, V.K. Pal, K. Kannan, *JECE*, **2021**, *3*, 91–116. [Crossref], [Google Scholar], [Publisher]

[4] R.A. Senthil, A. Selvi, P. Arunachalam, L.S. Amudha, J. Madhavan, A.M. Al-Mayouf, *J. Mater. Sci. Mater*, **2017**, *28*, 10081–10091. [Crossref], [Google Scholar], [Publisher]

[5] Y. Na, C. Chen, *Angew. Chem. Int. Ed*., **2020** *58,* 7629–7643. [Crossref], [Google Scholar], [Publisher]
[6] D.H. Liu, H.L. He, Y.B. Zhang, Z. Li, *ACS Sustainable Chem. Eng*., **2020**, *8*, 14322-14329. [Crossref], [Google Scholar], [Publisher]
[7] T. Ura, D. Shimbo, M. Yudasaka, N. Tada, A. Itoh, *Chem Asian J*., **2020**, *15*, 4000-4004. [Crossref], [Google Scholar], [Publisher]
[8] I. Vallés, L. Santos-Juanes, A.M. Amat, J. Moreno-Andrés, A. Arques, *Water*, **2021**, *13*, 1315. [Crossref], [Google Scholar], [Publisher]
[9] S. Nikhil, A. Karthika, P. Suresh, A. Suganthi, M. Rajarajan, *Adv Powder Technol*., **2021**, *32*, 2148-2159 [Crossref], [Google Scholar], [Publisher].
[10] P. Xiao, Y. Liu, W. Zong, J. Wang, M. Wu, J. Zhan, X. Yi, L. Liu, H. Zhou, *RSC Advances*, **2020**, *10*, 6801–6806. [Crossref], [Google Scholar], [Publisher]
[11] M. Zheng, J. Zhu, R. Fan, Y. Wang, Z. Lv, Y. Han, J. Peng, X. Zheng, R. Lin, *J. Braz. Chem. Soc.,* **2020**, *31*. [Crossref], [Google Scholar], [Publisher]
[12] N.S.T. Al-Awadie, M.H. Alalooshialamri, *Iraqi J. Sci*., **2015**, *56*, 875-897. [Pdf], [Google Scholar], [Publisher]
[13] I.M. Shakir Ali, N. Shakir, Turkey , A. A. H. Fares, *J. Phys.: Conf. Ser.,* **2021**, *2063*, 012031. [Crossref], [Google Scholar], [Publisher] .
[14] T. Artunc, A. Menzek, P. Taslimi, I. Gulcin, C. Kazaz, E. Sahin, *Bioorg. Chem*., **2020**, *100*, 103884. [Crossref], [Google Scholar], [Publisher]
[15] S. Zheng, J. Yan, K. Wang, *Engineering,* **2021**, *7*, 22-32. [Crossref], [Google Scholar], [Publisher]
[16] N. Ghasemi, M. Goodarzi, M. Khosravi, **2014**, *32*, 895-900. [Crossref], [Google Scholar], [Publisher].
[17] Analytical Methods Committee AMCTB No. 110, *Anal. Methods*, **2022**, *14*, 678-680. [Crossref], [Google Scholar], [Publisher].

How to cite this article: Sarah Faris Hameed*, Nagham Shakir Turkie. Determination of catechol by continuous flow injection analysis via turbidmetric utilizing NAG-4SX3-3D analyzer**.** *Eurasian Chemical Communications*, 2022, 4(8), 790-805. **Link:** http://www.echemcom.com/article_148175.html